Molecular-dynamics studies of grain-boundary diffusion. I. Structural properties and mobility of point defects

Thomas Kwok and Paul S. Ho
IBM Thomas J. Watson Research Center, Yorktown Heights, New York 10598

Sidney Yip
Department of Nuclear Engineering, Massachusetts Institute of Technology, Cambridge, Massachusetts 02139
(Received 22 December 1983)

The structural relaxation of a high-angle grain boundary at elevated temperatures has been simulated by molecular dynamics with the use of a bicrystal model composed of 399 atoms. The system studied was a $\Sigma=5$ (36.9°), [001] tilt boundary with interatomic interactions given by the empirical Johnson potential for α-Fe. In the presence of an extrinsic vacancy, the boundary structure was found to be stable up to temperatures of at least two-thirds the melting temperature. Vacancy jumps, confined preferentially to within the grain-boundary core, were observed. Also observed were the thermal activation of vacancy-interstitial pairs, and with increasing temperatures a variety of more complicated vacancy-jump sequences. The simulation data are relevant to the understanding of fast diffusion along grain boundaries, the kinetics of which is analyzed and discussed in the following paper.

I. INTRODUCTION

Atomic diffusion along grain boundaries (GB) is an important metallurgical process because it is often the dominant mechanism for matter transport in solids. Because the process is anisotropic and, by its very nature, strongly dependent on the local structure, the detailed relationship between GB structure and diffusion kinetics is a subject of considerable basic interst.[1-3] At temperatures appreciably below melting, it is believed that GB diffusion occurs by means of a point-defect exchange mechanism in a manner similar to atomic diffusion on a crystalline lattice.[4] On the other hand, GB diffusion is necessarily more complicated because, unlike a perfect lattice where every site is equivalent, there exist a number of distinct sites in the GB core, each having its characteristic binding energy for point defects and therefore contributing differently to atomic migration.

While the significance of structure in GB diffusion has been recognized, the way in which local structure affects atomic motion is still poorly understood. One main reason is that it is difficult experimentally to observe details of atomic migration in samples of known structure.[5] Another complication can arise in determining a diffusion mechanism when structural disorder sets in at elevated temperatures such that point defects are no longer well localized. When this occurs, even more information about local configurations will be needed in order to describe the diffusion process.

In the absence of appropriate experimental techniques, computer simulations have been used to generate equilibrium GB structures. Molecular-statics calculations valid at zero temperature have been carried out,[6] and results have been compared with experimental diffraction data.[7] This technique also has been applied to study configurations of various bicrystals in which a single vacancy has been introduced.[8] However, the approach cannot give direct information about GB structural stability at finite temperatures; also, it cannot be used to determined atom or defect migration rates. What is needed, therefore, is a simulation technique capable of generating atomic trajectories in a fully dynamic medium.

Molecular dynamics (MD) is a well-established technique for studying diffusion in liquids.[9] Using this method one can calculate the self-diffusion coefficient D, as well as obtain more microscopic details such as the mean-square displacement of an atom and its velocity autocorrelation function, both essential properties for understanding the basic nature of the diffusion process. The MD technique is equally suitable for solids, although thus far only limited studies of diffusion have been made.[10-12]

The purpose of this and the following paper is to present the results of a MD investigation of vacancy migration in a high-angle tilt boundary in a bcc structure. The system studied was a $\Sigma=5$ (36.9°), [001] tilt boundary in the (310) plane of α-iron. Vacancy jumps have been observed at several temperatures and the data provided direct evidence that vacancy exchange is the dominant mechanism governing GB diffusion. It was found that the vacancy-jump rate was higher in the GB core than in the bulk region, the jumps were anisotropic, favoring diffusion along the tilt axis, and the value of the activation energy for vacancy migration extracted from the data was quite reasonable. An unanticipated result was the thermal activation of boundary interstitials which were found to be immobile. Generally speaking, the present results confirm one's intuition that GB diffusion must be a highly structure-dependent phenomenon.

The organization of the papers is as follows. In the next section we describe the GB model and the simulation procedures used. In Sec. III we discuss structural stability at finite temperatures. In Sec. IV the properties of a lo-

calized vacancy in the present GB model are examined, and a procedure for defining a vacancy jump given. Section V describes the observation of thermal activation of Frenkel pairs which resulted in the production of a certain type of GB interstitial. The data show that this type of interstitial is short-lived and effectively immobile. The paper then concludes with some discussions. In the following paper we present the results on diffusion kinetics.

II. MODEL SYSTEM AND SIMULATION PROCEDURES

The grain boundary chosen for simulation is a $\Sigma=5$ coincidence site lattice tilt boundary in a bcc bicrystal generated by a rotation of 36.9° about an axis along [001]. Figure 1(a) shows the orientation of the bicrystal with its tilt axis along [001], and the boundary plane along [310]. The bicrystal is more easily recognized by its projection on the x-y plane; Fig. 1(b) shows two periods of the coincidence site boundary with atoms forming the "kite"-like figures occupying the lattice sites in the GB core region. The bicrystals are clearly periodic along the y direction, [310], with a period defined by the "kite"-like structure. It is also periodic along the z direction, [001], with a period of two atomic layers (cf. Fig. 4).

The simulation system is a stack of ten layers of (001) atomic planes, as shown in Fig. 1(a), with 40 atomic sites on each layer, as shown in Fig. 1(b). Periodic border conditions are applied along the y and z directions to take advantage of the inherent periodicity of the bicrystal. Along the x direction a fixed border condition is used since with periodic borders another grain boundary would be created. As shown in Fig. 1(b), additional atoms located beyond the x borders of the simulation system are introduced; these are allowed to interact with the atoms in the simulation system but they themselves are held rigid throughout the simulation.

All the atoms in the simulation system are assumed to interact via a two-body central potential. A number of empirical potential functions for bcc Fe are available,[13] the one chosen for this work is that constructed by Johnson.[14] The atomic trajectories are generated by integrating Newton's equations of motion using a fifth-order predictor-corrector method.[15,16] Prior to molecular-dynamics runs, the initial configuration for the simulation was prepared by molecular-statics relaxation.[8] The system was allowed to relax, then an extrinsic vacancy was introduced by removing an atom in the GB core and the minimum internal energy configuration again calculated. It was found that the relaxed GB structure prior to the insertion of the vacancy was characterized by a rigid-body expansion of one crystal relative to the other along the x direction by an amount $0.18a_0$, a_0 being the lattice constant. The system did not expand along the other directions, although such expansions were allowed to occur. The free volume in the boundary core created by this procedure was $V_f=0.82\Omega$ per boundary period in each layer, where $\Omega=0.34a_0^3$ is the volume occupied by an atom based on a hard-sphere model. Here V_f is the excess volume of the GB system over the volume of the perfect crystal containing the same number of atoms. When

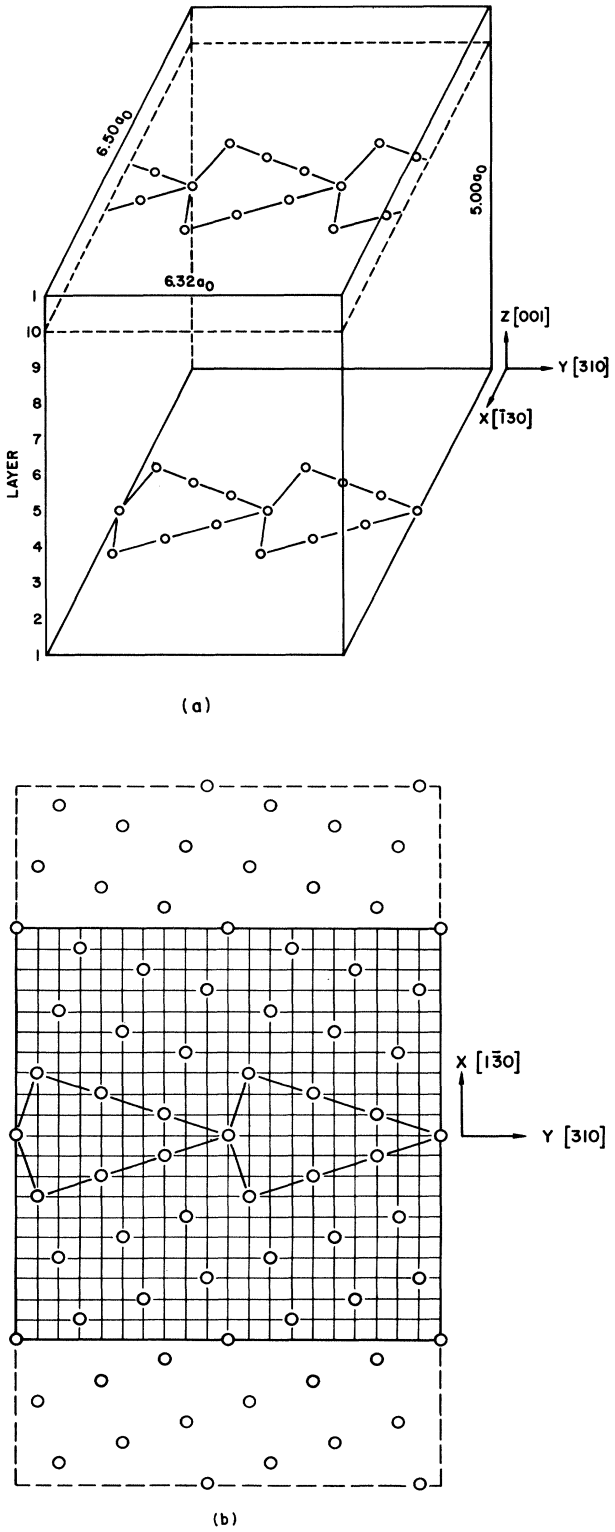

FIG. 1. The bicrystal model for molecular dynamics simulation: $\Sigma=5$ (36.9°), [001] tilt boundary in the (310) plane. (a) View showing stacking of ten (001) atomic planes. (b) View of one of the (001) planes with 40 atoms. Also shown are the fixed atoms in the border regions enclosed by dashed lines. Each unit of the fine square grid is equal to 2 DSC (displacement shift complete) (Ref. 27) unit ($0.32a_0$). The kite-shaped structure is composed of atoms belonging to the grain-boundary core.

the vacancy was introduced, the atoms in its vicinity underwent displacements considerably greater than they would in the bcc iron lattice; however, the vacancy remained well localized.

The initial configuration for the GB model produced by molecular-statics relaxation was verified to be an equilibrium structure at 0 K by molecular-dynamics simulation. Each atom in the system was given a small random velocity and the equations of motion integrated over several hundred time steps. If the system had not been relaxed sufficiently, there would be residual forces on some of the atoms which would then move and cause the system temperature to increase. When the simulation was carried out in this manner, the system temperature remained close to its initial value, indicating the configuration was indeed at equilibrium in the sense of zero net forces on the atoms.

To bring the system up to finite temperatures, the atoms were placed in the statically relaxed configuration and given velocity samples from a Maxwellian distribution characterized by a temperature T. After the simulation began, the system temperature quickly dropped from its initial value T to a value approximately $T/2$, as a result of the roughly equal partitioning of the input energy between kinetic and potential. This process took place in about 100 time steps, the time-step size Δt being about $\sim\frac{1}{40}$ of an atomic vibrational period. To allow time for equilibration, typically the first 500 time steps or more were not considered in the data analysis. In going from one temperature to another, the particle velocities were rescaled and the system given time to equlibrate.

Since the system volume was held fixed during simulation, it was necessary to adjust the volume in changing from one temperature to another in order to maintain approximately constant pressure. Volume adjustment was achieved by carrying out several short simulation runs at different temperatures to obtain an estimate of the coefficient of thermal expansion. The value deduced was $\sim 2\times 10^{-5}$ K.

The study of vacancy motions requires that the vacancy remain sufficiently localized and a procedure for determining when a jump event has actually occurred. For simulations up to ~ 1600 K the vacancy-free volume (assuming a hard-sphere model) was found to be greater than 0.6Ω during most of the time in between jumps. Under such conditions there was no difficulty in locating the vacancy during trajectory analysis. The procedure adopted for defining a jump event was to assign to each lattice site a spherical volume V' whether or not the site was occupied. A successful jump was considered to have taken place when an atom moved into the volume V' surrounding an empty (vacancy) site and stayed within V' for a period of at least two lattice vibrational periods. This procedure, which seemed quite arbitrary at first, evolved from detailed observations of how a localized free volume actually migrated from one site to another. The process would begin with the free volume undergoing a series of distortions until it had dispersed into two or more pieces, then the pieces would coalesce at a lattice site in a time on the average equal to or less than two vibrational periods.

From time to time an atom would move out of and back into the spherical volume assigned to its lattice site without being in another volume V' for any appreciable amount of time. Such events were treated as unsuccessful jumps with large displacement amplitudes. The requirement of a minimum vacancy residence time was intended to filter out from the data-analysis events in which a forward jump was quickly followed by a reverse jump, thus producing no net vacancy or atom displacements. It is clear that whatever the operational definition of jump event used, it would have an influence on the outcome of the data analysis such as the number of jumps and the residence time. Several different criteria were considered; the one chosen here appeared to be effective in minimizing the contribution of the exchange-reexchange jump processes.

III. GRAIN-BOUNDARY STABILITY AT ELEVATED TEMPERATURES

As the temperature of simulation is increased, the stability of the GB structure against thermal agitation has to be considered. An indication of onset of structural changes is given by the temperature variation of the system internal energy. As shown in Fig. 2 the internal energy followed a linear behavior up to ~ 1700 K where an abrupt increase occurred with further temperature increases. Since one is close to the experimental melting point of ~ 1800 K for iron, it is tempting to interpret the behavior between 1700 and 1800 K as a premelting transition. To reinforce this interpretation, we will consider other MD observations related to structural integrity, amplitudes of atomic vibration, and defect production.

Figure 3 shows the atomic positons in several (001) planes at different temperatures. The positions have been time-averaged over five lattice vibrational periods using the data taken from trajectories during an early part of the simulation. In the case of $T=1300$ K the vacancy originally inserted into layer 5 has moved to layer 9 where it is seen to be very well localized. The two adjacent layers are also shown, there being no observable distortion in the structure when compared to other layers in the sys-

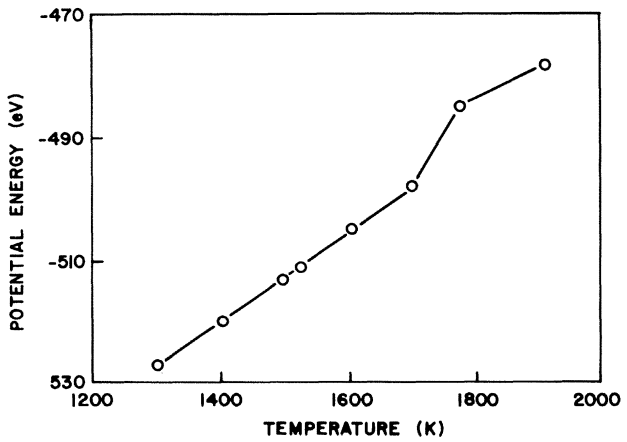

FIG. 2. Temperature variation of potential energy per atom of model bicrystal obtained by molecular-dynamics simulation with the pressure roughly held constant.

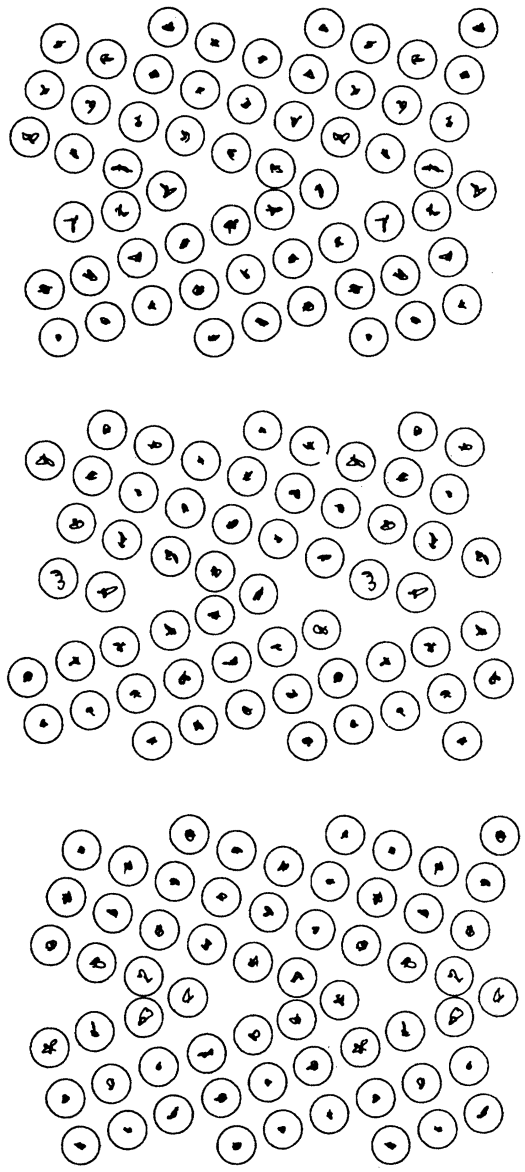

FIG. 3. Atomic configurations (circles) and displacement amplitudes (tracer plot) projected on the (001) plane in three adjacent layers which have been time-averaged over five lattice vibration periods at $T=1300$ K. The vacancy is in the middle layer.

tem. This type of structural rigidity persisted up to ~ 1600 K.

It is not surprising that the amplitudes of atomic motion in the GB are appreciably larger than in the bulk region. It can be observed in Fig. 3 that some of the GB atoms did experience greater than average displacements. This behavior shows up clearly in the mean-square displacement function

$$\langle r^2(t)\rangle = \frac{1}{N}\sum_{i=1}^{N}[\vec{r}_i(t)-\vec{r}_i(0)]^2 ,$$

where $\vec{r}_i(t)$ is the position of atom i at time t. For atoms which only vibrate about their equilibrium positions, $\langle r^2(t)\rangle$ approaches a constant value $\Delta^2 r$ at long times. Thus, $(\Delta^2 r)^{1/2}$ is a measure of the average size of the thermal cloud associated with atomic vibrations about a lattice site. Table I gives the displacement amplitudes of atoms in the GB region and those for atoms in the bulk. The division of GB and bulk is somewhat arbitrary since boundary thickness is itself not well defined. We have taken the GB region to be that indicated in Fig. 1(b); this choice gives 14 GB atoms and 26 bulk atoms in each layer except for the layer containing the extrinsic vacancy.

The results given in Table I are expressed as percentages of the nearest-neighbor separation which is $\sqrt{3}\,a_0/2$. One can see that starting at $T_m/2$, with T_m taken to be 1800 K, the average displacement of GB atoms is about 20% larger and the increase of $(\Delta^2 r)^{1/2}$ with temperature is also more rapid. The long-time behavior of $\langle r^2(t)\rangle$ could be determined reasonably well from relatively short simulations of 5000 time steps or less for T up to ~ 1700 K. Beyond this, the present data are no longer reliable. At $T=1913$ K, diffusion has set in among the GB atoms, and even though we will show a result for the bulk atoms, it is no more significant than just a short-time estimate. Thus, we see that the displacement amplitude data are consistent with the internal energy results.

The process of thermal point-defect production is clearly related to structural stability. In its initial state at $T=0$ K, the GB model contained an extrinsic vacancy in a relaxed configuration. When the system was brought into equilibrium at an evaluated temperature, it was expected that the vacancy migration would be thermally activated. It is also possible that during the simulation, other point defects could be spontaneously produced in the system. The probability of defect production will increase with the system temperature; however, its presence does not necessarily imply structural changes in the system.

In the range of temperatures studied we have observed not only a series of jumps by the extrinsic vacancy, but also the production of one or more Frenkel pairs. As might be expected, there were special sites in the GB core associated with which the defect formation energies were particularly low. The MD results revealed that a special site exists in the GB core which was especially favorable for the activation of an interstitial. Thus, when an atom jumped into this site, a Frenkel pair was created. Once created, the boundary interstitial was free to migrate until it encountered a vacancy and suffered annihilation. Further details of the interstitial mobility will be discussed in a later section.

TABLE I. Average atomic vibrational amplitude of atoms in the bulk and GB regions, in units of percent of nearest-neighbor separation, $\sqrt{3}a_0/2$.

T (K)	$[(\Delta^2 r)^{1/2}]_{\text{bulk}}$	$[(\Delta^2 r)^{1/2}]_{\text{GB}}$
910	8.5	10.2
1105	9.7	11.8
1307	10.6	13.7
1526	12.1	15.9
1698	13.2	17.9
1913	14.1	

TABLE II. Distribution of defect concentration during simulation expressed as fraction of time when there are V vacancies and I interstitials in the system.

V	I	1300 K	1400 K	1500 K
1	0	87.4	73.1	61.0
2	1	11.4	19.3	27.7
3	2	1.1	6.5	8.7
4	3	0.1	1.0	2.2
Others		0	0.1	0.4

Table II shows the distribution of defect concentration during simulation at different temperatures. At 1300 K, most of the time there was just one vacancy in the system, presumably the extrinsic vacancy, although a Frenkel pair was present about 11% of the time. Generation of Frenkel pairs increased significantly, however, with only moderate temperature increases. At 1700 K, the production of thermal defects reached such proportions that it became difficult to analyze the trajectory data for this information.

IV. VACANCY–GRAIN-BOUNDARY INTERACTIONS

The interpretation of vacancy migration data involves consideration of the static interactions between the vacancy and the GB system. We have previously noted that the various sites in the GB core are not equivalent so far as point-defect generation and subsequent motion are concerned. This property can be expressed quantitatively in terms of the formation and binding energies of vacancies and interstitials. The formation energy of a vacancy in a perfect lattice is defined as the energy of a vacancy minus the energy of a surface atom,

$$E_L^F(V)=E_L'(N-1)-E_L'(N) -\tfrac{1}{2}[E_L(N-1)-E_L(N)] ,$$

where $E_L(N-1)$ and $E_L(N)$ are the potential energies of the lattice with and without the vacancy, and the prime denotes relaxed configuration. Here it is assumed that the surface atom energy is half of that for an atom in the bulk. In a GB system the vacancy formation energy at a given site is similarly defined,

$$E_B^F(V)=E_B'(N-1)-E_B'(N) -\tfrac{1}{2}[E_L(N-1)-E_L(N)] .$$

The vacancy binding energy is then given by

$$E_B^B(V)=E_B^F(V)-E_L^F(V) .$$

The results of the vacancy formation and binding energies calculated by molecular statics are given in Table III for the various sites labeled in Fig. 4. Since configuration relaxation also can be carried out by molecular dynamics, we have verified in one case that the two methods indeed gave the same result. Figure 4 shows one (001) layer and the projection of an adjacent layer. There are four different sites, A, B, C, and D, in the eight-atom kite-shaped figure (primes denote equivalent sites which constitute what might be considered the GB core). The unlabeled sites are assumed to behave like the bulk lattice or L site. The ratio of sites in our model is therefore

$$A:B:C:D:E:F:G:L = 1:2:2:2:2:2:2:7 .$$

TABLE III. Formation and binding energies of vacancies and interstitials at sites in the GB core.

	Site	E_B^F (eV)	E_B^B (eV)
Vacancies	A	1.33	−0.02
	B	0.94	−0.41
	C	1.26	−0.09
	D	1.17	−0.18
Interstitials	I	1.06	−3.68
	A	2.55	−2.19
	B	2.55	−2.19
	C	3.30	−1.44
	D	2.32	−2.42

In the division of the system into GB and bulk regions, sites E, F, and G are also assigned to the bulk region even though their formation and binding energies are different from the L site. One sees from Table II that vacancy formation energies for the different sites can differ by as much as ~40%, and with E_L^F determined to be 1.35 eV there is a wide range of variation in the binding energies. The low value of E_B^F for site B means that the system can lower its energy the most by having a vacancy in a neighboring site jump into B. The values of E_B^F, or correspondingly E_B^B, will be used later to correlate with the observed jump frequencies for each site. Since the static energies reflect the different distribution of neighbors one can analyze the results of Table II in terms of the various neighbor distances. From Table III it is seen that the shortest distances are $B-B'$.

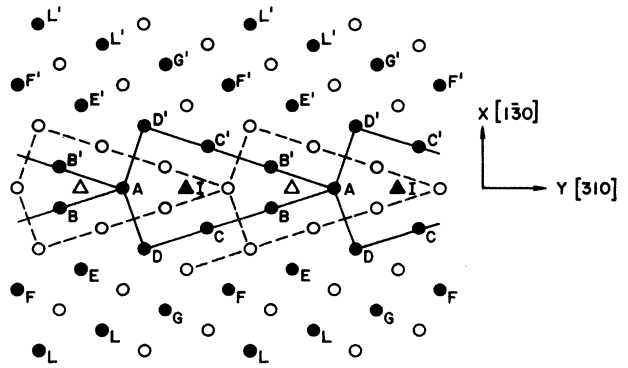

FIG. 4. An (001) atomic plane (solid symbols) with projection of an adjacent plane (open symbols). Various discrete sites are labeled for later discussions of vacancy formation and migration. The boundary interstitial site is indicated by the triangle and labeled as I. Primed and unprimed atom sites are equivalent, and L refers to a lattice site.

V. INTERSITIAL FORMATION AND MOBILITY

An interstitial can be inserted into the GB model by simply putting an extra atom into a preselected position and allowing the system to relax. The resulting configurations and static energies of the interstitial have been investigated by means of molecular-statics calculations.[8] An interstitial was inserted into position I in Fig. 4 which, based on a hard-sphere model consideration, was the largest "hole" in the GB core. Considerable relaxation occurred around the interstitial, but it remained easily recognizable as an extra atom. Interstitials were also introduced at sites A, B, C, and D. This was done by displacing the atom originally on the site and letting it and the extra atom form a dumbbell with its center positioned at the site location. The relaxed configurations showed some delocalization, still the dumbbell pair remained as a *bona fide* point defect in the GB structure.[17]

The interstitial formation energy is defined as the energy of an interstitial plus the energy of a surface atom. The former is calculated from the difference in the potential energies of the relaxed configurations with and without the interstitial. For the perfect lattice the formation energy is

$$E_L^F(I)=E_L'(N)-E_L'(N+1)+\tfrac{1}{2}[E_L(N-1)-E_L(N)]\ ,$$

whereas for the GB system it is

$$E_B^F(I)=E_B'(N)-E_B'(N+1)+\tfrac{1}{2}[E_L(N-1)-E_L(N)]\ .$$

The binding energy of an interstitial in the GB is determined by

$$E_B^B(I)=E_B^F(I)-E_L^F(I)\ .$$

Results for the formation and binding energies are given in Table III; these are useful for understanding the simulation data.

In the course of MD simulation various defects were created by fluctuations in atomic displacements as a result of thermal motions. The thermal activation of a particular type of boundary interstitial was observed in the present study. It was found that an atom on site A, B, or C would jump into site I in the manner shown in Fig. 5. A procedure similar to that devised to define vacancy jumps was followed to define an interstitial formation and determine when such an event occurred. The same spherical volume V' was assigned to each interstitial site I. When an atom moved into this volume and stayed in it for more than a vibrational period, a boundary interstitial was considered to be created and at the same time a vacancy was formed at the site previously occupied by the atom. Since the separation distance between the GB site B and the interstitial site I was $0.64a_0$, which was less than $\frac{9}{10}$ of the nearest-neighbor distance of $0.86a_0$, an atom could lie within both volumes assigned to the two sites. When this occurred, the atom was always considered as belonging to the GB site because the atom was more stable at the lattice site than at I. In view of the shorter jump distance between B and I compared to a vacancy-jump distance, the minimum residence time for interstitial formation was taken to be one vibrational period.

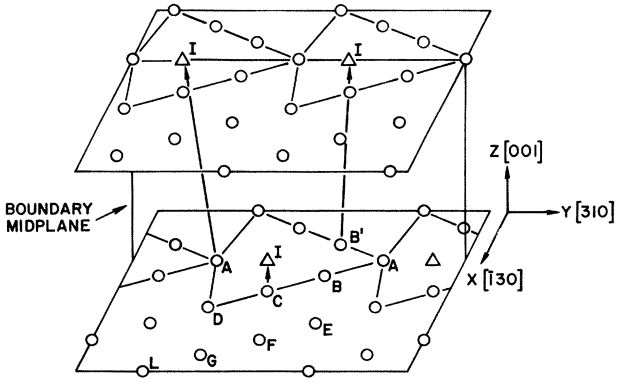

FIG. 5. Three different sequences of thermally activating a Frenkel pair with interstitial at I and vacancy at site A, B, or C that have been observed.

The processes depicted in Fig. 5 correspond to the spontaneous creation of Frenkel pairs. Table II shows the likelihood of observing one or more such Frenkel pairs at the three temperatures studied. It is not surprising that the probability of defect generation increases with temperature in both single and multiple defects. The number of interstitials at site I motivated from the different GB sites is given in Table IV, the relative proportions being consistent with the jump distances $B-I=0.64a_0$, $C-I=0.80a_0$, and $A-I=0.81a_0$. Notice that as the temperature increased, the effect of site preference decreased, as expected.

The effective formation energy of a Frenkel pair with interstitial at site I may be extracted from the simulation data by plotting the effective defect concentration, $\tilde{n}(V-I)$, as in Fig. 6. The results can be fitted reasonably well by the form

$$\tilde{n}(V-I)=\exp(\Delta\tilde{S}_{V-I})\exp[-\tilde{E}_B^F(V-I)/k_BT]$$

with effective formation energy $\tilde{E}_B^F(V-I)=1.08$ eV and effective entropy increase $\Delta\tilde{S}_{V-I}=2.40$. The value of $\Delta\tilde{S}_{V-I}$ is in the range generally expected for the increase in entropy in pure metals when a vacancy or an interstitial is introduced. The value of $\tilde{E}_B^F(V-I)$ can be compared with that obtained from static calculations such as those shown in Table III.

TABLE IV. Distribution of interstitials thermally activated from various GB sites.

T (K)	A	B	C
1300	2	130	9
1400	8	208	27
1500	30	341	44

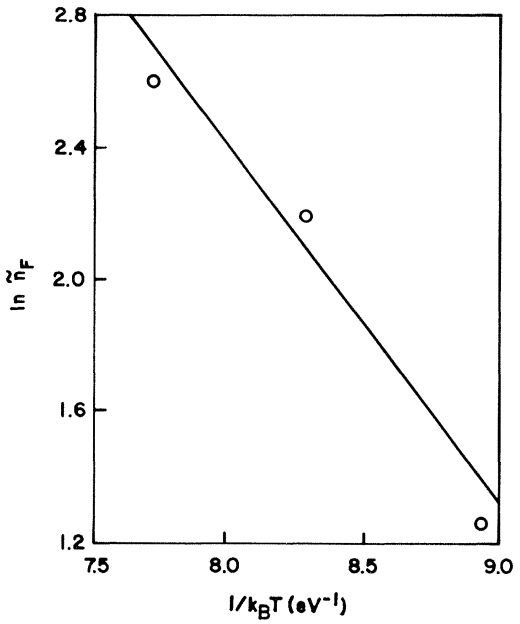

FIG. 6. Observed temperature dependence of activated Frenkel-pair concentration.

The vacancy formed in the Frenkel pair occasionally diffused away, leaving behind the interstitial trapped at site I. During its lifetime the interstitial was found to be immobile. At the end of its lifetime, it annihilated with a vacancy which could be its original partner or another vacancy which happened to be in the vicinity. As shown in Fig. 7, interstitials are short-lived; half of these defects had lifetimes less than one vibrational period and therefore qualified best as stable interstitials.

The explanation of the occurrence and immobility of the interstitial at site I lies in the significantly lower formation energy, as given in Table III. Using the vacancy and interstitial formation eneriges from Table III, one obtains the binding for the Frenkel pair (in units of eV)

$$E_B^B(V-I)=E_B^F(V)+E_B^F(I)-E_B^F(V-I)=0.98\ .$$

The high value of the binding energy accounts for the immobility of the interstitial.

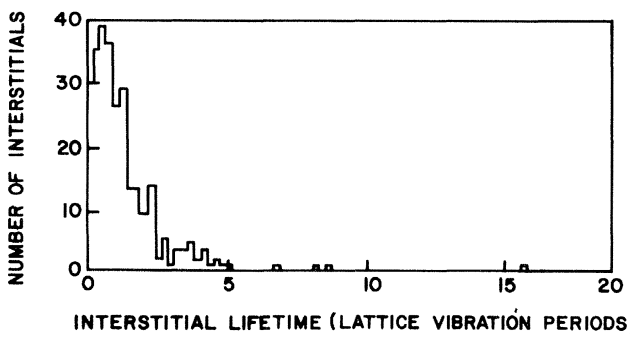

FIG. 7. Distribution of boundary interstitial lifetime at $T=1300$ K.

VI. HIGHER-ORDER JUMP PROCESSES

Analysis of the present MD trajectories has revealed a number of multiply correlated jump sequences during the various simulations. The observation of these less frequent, higher-order jumps means that defect motions at elevated temperatures cannot be described only in terms of monovacancy jumps. The processes observed include the direct interchange of two closely packed atoms, the double jump in which two atoms jump in unison, the indirect jump where a vacancy effectively migrated to a site two boundary planes away, and other vacancy jumps over distances greater than the nearest-neighbor separations.

Figure 8 shows the interchange of atoms at B and B' via a ring mechanism which involved two interstitial sites. In this four-step process, atoms in adjacent sites B and B' jumped, one after the other, into sites I in the boundary planes above and below. Then the interstitials created at I jumped into the empty sites of each other at approximately the same time. The sequence on the left of Fig. 8 shows an observed interchange of atoms at B and B' involving only one interstitial site I. In this process, which results from three consecutive jumps, an atom at B jumped into I in the adjacent boundary plane, followed by an atom at B' jumping into the just-created vacancy at B, and the sequence completed by the interstitial at I jumping into the vacancy at B'. Occurrence of both processes was found to increase with temperature, with the process involving two interstitial sites dominating at low and intermediate temperatures. That means given an atom in site B and a vacancy in adjacent site B', the atom will most likely jump first to an interstitial site I in the adjacent boundary plane, the most likely sequence being B-I-B'. This preference is consistent with the B-I separation distance of $0.64a_0$ as compared to the B-B' separation of $0.84a_0$. Since the two atoms involved are, in effect, still

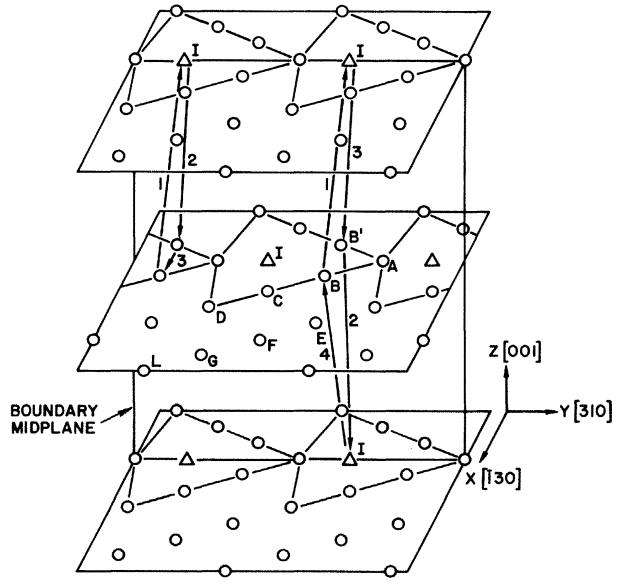

FIG. 8. Two observed atomic-jump sequences resulting in the direct interchange of closely packed atoms at B and B'. The numbers indicated the sequence of jumps.

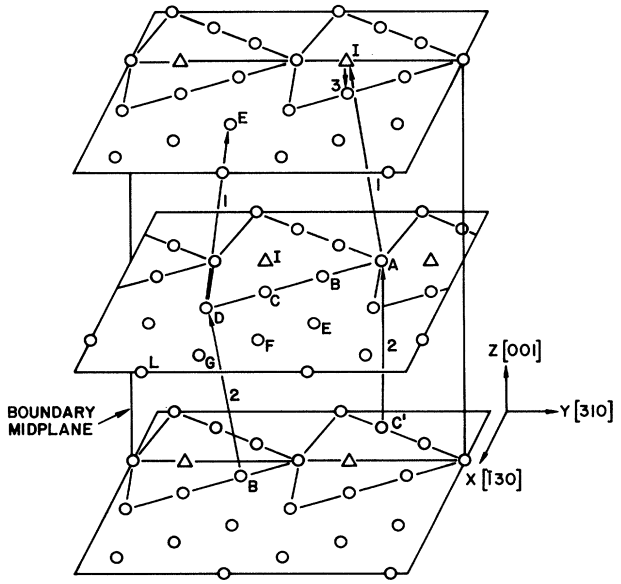

FIG. 9. Observed jump sequences showing a double jump (left) and an indirect jump (right). The numbers indicated the sequence of jumps.

trapped in the same pair configuration, neither process contributes to self-diffusion.

At high temperatures, the double jump depicted in Fig. 9, was observed. This process has been previously reported in MD simulation of self-diffusion in Na and K near their melting points.[11] The effect of the double jump is to transport the vacancy to a site two boundary steps away. A related process is the indirect jump, which is also illustrated in Fig. 9. In this case, an atom at A jumped to I in the boundary plane above, which contained a vacancy at B, followed by an atom at C' in the boundary plane below jumping into the newly created vacancy at A. Then the interstitial at I jumped into B, resulting in a net vacancy displacement from B to C' two boundary planes away.

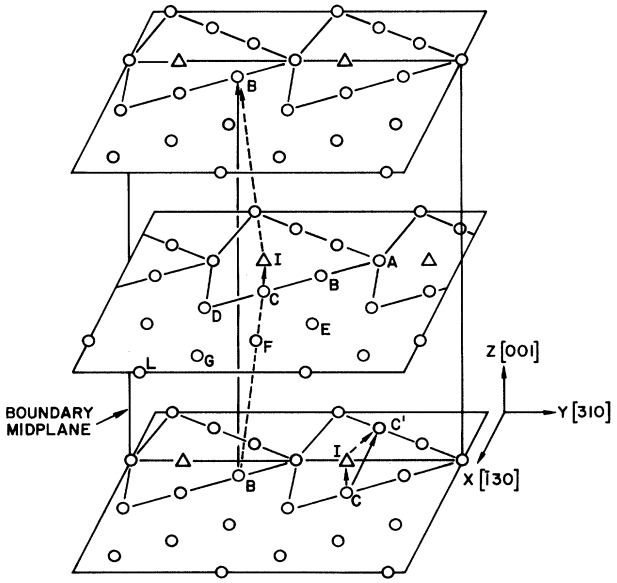

FIG. 10. Two observed sequences showing vacancy jumps over distances greater than nearest-neighbor separation.

At temperatures near melting, jumps were observed which extended over distances greater than the nearest-neighbor separation of $0.87a_0$. Figure 10 shows examples of jumps over second and third nearest-neighbor distances, B-B and C-C' processes. Notice that in each case the process occurred in two steps, with the interstitial site I serving as a link between different GB sites. These are events which may be expected at elevated temperatures. Although they have been observed in the present study, further simulations are necessary to compile sufficient statistics before quantitative information can be deduced.

VI. DISCUSSION

In this work we have attempted to show that MD offers unique advantages in investigating the behavior of defect structures at finite temperatures. In the absence of experimental techniques capable of providing atomistic level information about defect kinetics, computer simulation can be an important tool for obtaining physical insights, one that can reveal both the effects associated with structure and those associated with dynamics. Unlike static calculations, MD allows the defect structure to evolve under all the forces that would be present in a thermodynamic system, and except for boundary conditions imposed at the borders of the simulation volume there are no constraints on the atoms. As a result one may observe at elevated temperatures structural changes and kinetic processes that would be difficult to anticipate *a priori*, and therefore difficult to study by static calculations. An example of the kind of unanticipated results that MD can produce is the formation of Frenkel pairs and the subsequent immobility of the resulting boundary interstitial.

It is relevant to ask whether the present results are also characteristic of other GB structures and interatomic interactions. A general answer can not be given because the effects of GB structure and interatomic forces on diffusion kinetics are still not sufficiently understood. On the other hand, we believe the qualitative features of vacancy migration we have observed should manifest also in other GB systems. This belief is supported by similar observations of Frenkel-pair formation in a fcc $\Sigma=5$ tilt boundary with Lennard-Jones interatomic potential.[18] Simulations of vacancy migration in aluminum bicrystals are currently in progress to ascertain the differences between fcc and bcc structures, and also the influence of different potential functions.

The concept of the point-defect exchange mechanism for diffusion requires the point defects to be well defined, which in turn requires the GB structure to be stable. As one approaches the melting point of the bulk lattice, one can expect the concept to become increasingly untenable because the point defects may not be well localized. Indeed local structural disorder can strongly affect defect formation and kinetics. The problem is further complicated by the possibility of premelting transition in the GB core which results in the onset of disorder at a temperature distinctly below melting. In Fig. 2 we have observed a sudden increase in the internal energy in the vicinity of

1700 K, and at the same time defect production was found to increase markedly. This may be regarded as an indication of a premelting transition.[19,20] More detailed evidence has been obtained recently from two separate MD studies, both involving bicrystals with Lennard-Jones interatomic potential. A study of the temperature variation of the enthalpy of a two-dimensional $\Sigma=7$ bicrystal has shown that a transition occurs approximately beteween $0.7T_m$ and $0.8T_m$.[21] More definitive results concerning local structure and diffusion properties, obtained from a three-dimensional $\Sigma=5$ bicrystal, indicate a continuous onset of disorder below the transition.[22] It is clear that computer simulations can play a leading role in elucidating the nature of this fundamental phenomenon. Further investigations will be of even greater value because local structure, thermodynamic properties, and defect formation and kinetics all can be studied within a single simulation.

In the following paper[23] we will examine in detail the simulation data on vacancy migration in the intermediate range of temperatures, and discuss their significance concerning diffusion mechanism and kinetics.[24] It is our goal to demonstrate, through a number of specific calculations such as the one presented here, that MD can produce invaluable information, data that can not be obtained by other means. In this respect it is worth noting that future work should incorporate a method for allowing simulations at constant pressure, or more generally at constant prescribed external stress.[25,26] Techniques such as the use of wave-vector-dependent density order parameter to describe local structural order and velocity autocorrelation function to measure the self-diffusion coefficient will also help to extract even more information from the atomic trajectories.

ACKNOWLEDGMENTS

We would like to acknowledge the collaboration of P. D. Bristowe, R. W. Balluffi, and A. Brokman, especially during the early phase of the work. A portion of the work carried out at Massachusetts Institute of Technology was supported by the U.S. Army Research Office.

[1]N. P. Peterson, in *Grain Boundary Structure and Kinetics,* edited by R. W. Balluffi (American Society of Metals, Metals Park, Ohio, 1980), p. 209; N. L. Peterson, Int. Metall. Rev. 28, 65 (1983).

[2]R. W. Balluffi, in *Grain Boundary Structure and Kinetics* (Ref. 1), p. 297; R. W. Balluffi, Metall. Trans. 13B, 527 (1982).

[3]H. Gleiter and B. Chalmers, *High-Angle Grain Boundaries* (Pergamon, New York, 1972).

[4]J. R. Manning, *Diffusion Kinetics for Atoms in Crystals* (Van Nostrand, New York, 1968).

[5]G. Martin and B. Perraillon, in *Grain Boundary Structure and Kinetics* (Ref. 1), p. 239.

[6]For a review see R. J. Harrison, G. A. Briggeman, and G. H. Biship, in *Grain Boundary Structures and Properties,* edited by G. A. Chadwick and D. A. Smith (Academic, New York, 1976), p. 45; V. Vitek, A. P. Sutton, D. A. Smith, and R. C. Pond, in *Grain Boundary Structure and Kinetics* (Ref. 1), p. 115.

[7]P. D. Bristowe and S. L. Sass, Acta Metall. 28, 575 (1980); P. D. Bristowe, J. Phys. (Paris) Colloq. 43, C6-33 (1982).

[8]A. Brokman, P. D. Bristowe, and R. W. Balluffi, J. Appl. Phys. 52, 6116 (1981).

[9]J.-P. Hansen and I. R. McDonald, *Theory of Simple Liquids* (Wiley, New York, 1976); W. W. Wood and J. J. Erpenbeck, Annu. Rev. Phys. Chem. 27, 319 (1976).

[10]C. H. Bennett, in *Diffusion in Solids,* edited by J. J. Burton and A. S. Nowick (Academic, New York, 1975), p. 73.

[11]A. Da Fano and G. Jacucci, Phys. Rev. Lett. 39, 950 (1977).

[12]G. de Lorenzi, G. Jacucci, and V. Pontikis, Surf. Sci. 116, 391 (1982).

[13]A. M. Stoneham and R. Taylor, *Handbook of Interatomic Potentials. II. Metals* (United Kingdom Atomic Energy Authority, Harwell, 1981) [Report No. AERE-R10205 (1981)].

[14]R. A. Johnson, Phys. Rev. 134, A1329 (1964).

[15]A. Rahman, Phys. Rev. 136, A405 (1964).

[16]O. Deutsch, Ph.D. thesis, Massachusetts Institute of Technology, 1975.

[17]P. D. Bristowe and R. W. Balluffi (private communication); see also Ref. 23.

[18]M. Guillope, Ph.D. thesis, University of Paris, 1982.

[19]H. Gleiter and B. Chalmers, Ref. 3, chapter on GB melting.

[20]A calculation based on lattice gas model which predicts GB melting has been reported by R. Kikuchi and J. W. Cahn, Phys. Rev. B 21, 1893 (1980).

[21]F. Carrion, thesis, Massachusetts Institute of Technology, 1982; F. Carrion, G. Kalonji, and S. Yip, Scr. Metall. 17, 915 (1983).

[22]G. Ciccotti, M. Guillope, and V. Pontikis, Phys. Rev. B 27, 5576 (1983).

[23]T. Kwok, P. S. Ho, and S. Yip, this issue, following paper, Phys. Rev. B 29, 5363 (1984).

[24]T. Kwok, P. S. Ho, S. Yip, R. W. Balluffi, P. D. Bristowe, and A. Brokman, Phys. Rev. Lett. 47, 1148 (1981); R. W. Balluffi, T. Kwok, P. D. Bristowe, A. Brokman, P. S. Ho, and S. Yip, Scr. Metall. 15, 951 (1981).

[25]H. C. Andersen, J. Chem. Phys. 72, 2384 (1980); J. M. Haile and H. W. Graben, *ibid.* 73, 2412 (1980).

[26]M. Parrinello and A. Rahman, J. Appl. Phys. 52, 7182 (1981).

[27]W. Bollmann, *Crystal Defects and Crystalline Interfaces* (Springer, Berlin, 1970).